

Universal monomer dynamics of a two dimensional semi-flexible chain

Aiqun Huang, Ramesh Adhikari, and Aniket Bhattacharya*

Department of Physics, University of Central Florida, Orlando, Florida 32816-2385, USA

Kurt Binder

Institut für Physik, Johannes Gutenberg-Universität Mainz, Staudinger Weg 7, 55099, Mainz, Germany

(Dated: August 9, 2013)

We present a unified scaling theory for the dynamics of monomers for dilute solutions of semi-flexible polymers under good solvent conditions in the free draining limit. Our theory encompasses the well-known regimes of mean square displacements (MSDs) of stiff chains growing like $t^{3/4}$ with time due to bending motions, and the Rouse-like regime $t^{2\nu/(1+2\nu)}$ where ν is the Flory exponent describing the radius R of a swollen flexible coil. We identify how the prefactors of these laws scale with the persistence length ℓ_p , and show that a crossover from stiff to flexible behavior occurs at a MSD of order ℓ_p^2 (at a time proportional to ℓ_p^3). A second crossover (to diffusive motion) occurs when the MSD is of order R^2 . Large scale Molecular Dynamics simulations of a bead-spring model with a bond bending potential (allowing to vary ℓ_p from 1 to 200 Lennard-Jones units) provide compelling evidence for the theory, in $D = 2$ dimensions where $\nu = 3/4$. Our results should be valuable for understanding the dynamics of DNA (and other semiflexible biopolymers) adsorbed on substrates.

PACS numbers: 82.35.Lr, 87.15.A-, 87.15.H-

Conformations and dynamics of semi-flexible polymers in bulk as well as under various applied fields, *e.g.*, confining and stretching potentials are of broad general interest in different disciplines of science. Important biopolymers, *e.g.*, dsDNA, F-Actin, microtubules, all have finite bending rigidity κ , often with large persistence lengths and hence the well established and matured theories for fully flexible chains often are not adequate to describe these biopolymers as flexural rigidity plays an important role in their mechanical responses [1]. Interests in these biopolymers continue to remain unabated for multiple reasons. (i) A deeper understanding of biopolymers, *e.g.*, Actin, Titin, Fibrin which offer intriguing patterns with unusual viscoelastic responses will allow to design bio-mimetic materials with improved characteristics, not seen in synthetic polymers; (ii) there is a genuine need to develop efficient separation methods of biomolecules, *e.g.*, DNA sequencing and separation of proteins for various applications pertaining to health and diseases. Finally, due to advent of sophisticated single molecule probes, *e.g.*, fluorescence correlation spectroscopy, atomic force microscope spectroscopy, scanning electron spectroscopy with which one can directly observe the dynamics of the entire chain as well as fluorescence labeled segments of these biomolecules [2]-[6] which offer new findings to be further explored.

Historically the worm-like chain (WLC) model has been the paradigm for theoretical studies of semi-flexible chains. The Hamiltonian for the WLC is given by

$$\mathcal{H} = \frac{\kappa}{2} \int_0^L \left(\frac{\partial^2 \mathbf{r}}{\partial s^2} \right)^2 ds, \quad (1)$$

where L is the contour length, κ is the bending rigidity and the integration is carried along the contour

s [7, 8]. One can show that in 2D and 3D dimensions $\ell_p = 2\kappa/k_B T$ and $\kappa/k_B T$ respectively [9]. The model has been studied quite extensively applying path integral and other techniques [10]-[17] and exact expressions of various moments of the distribution of monomer distances along the chain have been worked out. In particular, the end-to-end distance for the WLC model is given by [7]

$$\frac{\langle R_N^2 \rangle}{L^2} = \frac{2}{n_P} \left(1 - \frac{1}{n_P} [1 - \exp(-n_P)] \right), \quad (2)$$

where $L = (N-1)\delta$ is the contour length and $n_P = L/\ell_p$. Here we recall that any linear polymer is a chain molecule of N discrete monomeric units, and we take the distance between the neighboring units as δ . In the limit $n_P \gg 1$, *i.e.*, $\ell_p \ll L$ one gets $\langle R_N^2 \rangle = 2\ell_p L$ and the chain behaves like a Gaussian coil; for $n_P \ll 1$, $\langle R_N^2 \rangle = L^2$ and the chain behaves like a rod. Evidently the model neglects the excluded volume (EV) interaction and hence interpolates between rod and Gaussian limit. Dynamics of the WLC model has been explored using Langevin type of equation [14-18]. One can expect that the dynamics of a stiff-chain will be dominated by transverse fluctuations (bending modes) [13] and that the short time dynamics will be governed by the chain persistence length. Indeed a relaxation dynamics using the WLC Hamiltonian (Eqn. 1) approach yields an expression for fluctuation $\langle (\Delta h)^2 \rangle \sim \ell_p^{-0.25} t^{0.75}$, which crosses over to simple diffusion at late time [14, 15]. This $t^{0.75}$ behavior has been observed in many experiments using fluorescence probe and video microscopy on F-Actin network [2-4] and in some simulations of polymer network [19, 20]. Analytical studies of monomer dynamics in a WLC model, similar to [14, 15] have been carried out for a tagged particle by Bullerjahn *et al.* [18] who also found that the transverse

MSD of a tagged particle obeys subdiffusive behavior of $t^{0.75}$.

While these predictions based on WLC model are consistent with some of the experiments, the WLC model fails to capture important aspects caused by EV effects [21, 22] invalidating Eqn. 2 in the limit $n_p \gg 1$ both in 2D and 3D where the chain statistics in D spatial dimension satisfies [23, 24],

$$\sqrt{\langle R_N^2 \rangle} \sim N^\nu \ell_p^{1/D+2}. \quad (3)$$

The Gaussian regime of WLC model is completely absent in 2D [21]; in 3D the Gaussian regime crosses over at $\langle R_N^2 \rangle \sim \ell_p^3$ to 3D self avoiding walk (SAW) of Eqn. 3 [22]. Furthermore, the angular correlation between subsequent bonds along the chain, instead of exponential, as predicted by the WLC model, exhibits a power-law decay. Therefore, EV effect has a profound effect on the statistics of stiff chains as well.

A key question is then how the EV effect affects the monomer dynamics of a semiflexible chain. We have developed a scaling theory of monomer dynamics for a compressible semi-flexible chain. *We predict a novel double crossover dynamics where the initial sub-diffusive relaxation of the monomers characterized by a $t^{0.75}$ law at an intermediate time crosses over to the monomer dynamics of a flexible chain $t^{\frac{2\nu}{1+2\nu}}$ before reaching the purely diffusive regime for the entire chain.* This is the main theoretical result of this letter. We support our claim by carrying out extensive BD simulation for a large number of chain lengths from $N = 16$ to $N = 1024$ and $\kappa = 1.0 - 128$, to show that (i) $\langle R_N^2 \rangle / (2L\ell_p)$ as a function of L/ℓ_p for all ratios L/ℓ_p collapse on the same master plot and that the early time slope of unity ($\langle R_N^2 \rangle \propto L^2$; rod limit) directly crosses over to slope of 0.5 ($\langle R_N^2 \rangle \propto L^{1.5} \ell_p^{0.5}$; 2D SAW, Eqn. 3) clearly demonstrating absence of Gaussian regime in 2D. (ii) Second, by monitoring the dynamics of middle monomer $g_1(t) = \langle (\mathbf{r}_{N/2}(t) - \mathbf{r}_{N/2}(0))^2 \rangle$, and comparing it with that of the center of mass $g_3(t) = \langle (\mathbf{r}_{CM}(t) - \mathbf{r}_{CM}(0))^2 \rangle$, and the relative dynamics of $g_1(t)$ with respect to $\mathbf{r}_{CM}(t)$ expressed as $g_2(t) = \langle (\mathbf{r}_{N/2}(t) - \mathbf{r}_{CM}(t)) - (\mathbf{r}_{N/2}(0) - \mathbf{r}_{CM}(0))^2 \rangle$ [25–28] we show data collapse and monomer crossover dynamics. We believe these studies of chain conformation and monomer dynamics will be extremely valuable to interpret experimental results and testing certain approximations in analytical theories for semiflexible chains [11, 16, 17].

• *Scaling theory:* We start with the Eqn. 4 below derived by Granek and Maggs [14, 15] using a Langevin dynamics framework for the WLC Hamiltonian of Eqn. 1

$$g_1(t) = \delta^2 (\delta/\ell_p)^{1/4} (Wt)^{3/4}. \quad (4)$$

Here we have chosen the inverse of a monomer reorientation rate W^{-1} as the unit of time. For early time the monomer dynamics will be independent of the chain

length N until the fluctuations become of the order of ℓ_p . Therefore, denoting the first crossover occurs at time τ_1 and substituting $g_1 = \ell_p^2$ and $t = \tau_1$ in Eqn. 4 we immediately get

$$W\tau_1 = (\ell_p/\delta)^3. \quad (5)$$

For $0 < t \leq W^{-1}(\ell_p/\delta)^3$ the monomer dynamics is described by $g_1(t) \sim t^{0.75}$ until $g_1(t) = \ell_p^2$ at time $W^{-1}(\ell_p/\delta)^3$. The width of this region is independent of N and solely a function of ℓ_p .

For $\tau_1 < t < \tau_2$ the dynamics is governed by the Rouse relaxation of monomers of a fully flexible EV chain in 2D characterized by $g_1(t) = t^{2\nu/(1+2\nu)} = t^{0.6}$. τ_2 characterizes the onset of the purely diffusive regime when $g_1(\tau_2) = \langle R_N^2 \rangle$ [25]. We then obtain τ_2 as follows:

$$g_1(t) = \ell_p^2 (t/\tau_1)^{3/5} \quad \text{for } t > \tau_1. \quad (6)$$

Substituting τ_1 from Eqn. 5 in above

$$g_1(t) = \delta^2 (\ell_p/\delta)^{1/5} (Wt)^{3/5}, \quad \text{for } \tau_1 < t < \tau_2. \quad (7)$$

At $t = \tau_2$

$$g_1(t = \tau_2) = \langle R_N^2 \rangle = \ell_p^{1/2} \delta^{3/2} N^{3/2}. \quad (8)$$

Substituting Eqn. 7 for $t = \tau_2$ we get

$$W\tau_2 = (\ell_p/\delta)^{\frac{1}{2}} N^{5/2}. \quad (9)$$

We also note that the dynamics of the center of mass is given by (omitting prefactors of order unity throughout)

$$g_3(t) = \delta^2 W \frac{t}{N}. \quad (10)$$

The “phase diagram” for the crossover dynamics in terms of N , and ℓ_p are shown in Fig. 1. Notice that for a stiffer chain the region for $\tau_1 < t < \tau_2$ for which we predict $g_1(t) \sim t^{0.6}$ becomes progressively small and therefore, is hard to see in simulation for a stiffer chain.

• *BD simulation for a 2D EV semiflexible chain:* We have used a standard BD scheme using Lennard-Jones(LJ), finite extensible nonlinear elastic (FENE) [25] potentials to describe EV and spring potentials, and a three body potential among three consecutive monomers to describe chain stiffness as in [29, 30].

• *Absence of Gaussian regime and correct scaling for a 2D EV chain:* Fig. 2 shows a plot of $\langle R_N^2 \rangle / 2\ell_p L$ as a function of L/ℓ_p for a huge number of values of L/ℓ_p (~ 100). For $L/\ell_p \ll 1$ we observe that $\frac{\langle R_N^2 \rangle}{2\ell_p L} \sim (L/\ell_p)^{1.0}$ while for $L/\ell_p \gg 1$ the data very nicely fit with $\frac{\langle R_N^2 \rangle}{2\ell_p L} \sim (L/\ell_p)^{0.50}$. This plot for chains with varying degree of stiffness and chain length conclusively shows the absence of Gaussian regime in a 2D EV chain earlier observed by Hsu *et al.* from a lattice model [21] and observed

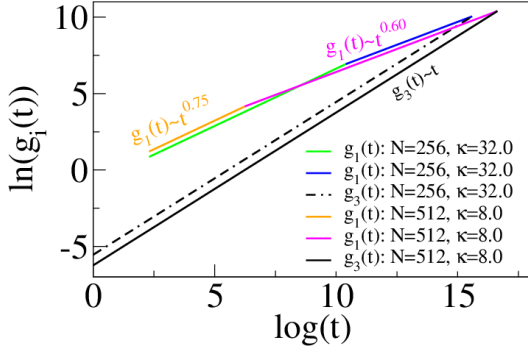


FIG. 1. Theoretical scaling plots for $(N, \kappa) \equiv (256, 32)$ and $(N, \kappa) \equiv (512, 8)$. Green and orange lines correspond to $g_1(t) \sim t^{0.75}$, blue and magenta lines correspond to $g_1 \sim t^{0.60}$, and the dashed and solid black lines correspond to $g_3(t) \sim t$ for $N = 256$ and 512 respectively. The width of each region shows how these regimes depend on ℓ_p and N . Note that in reality we expect a very gradual change of slope on the log-log plot at both crossover times, rather than sharp kinks.

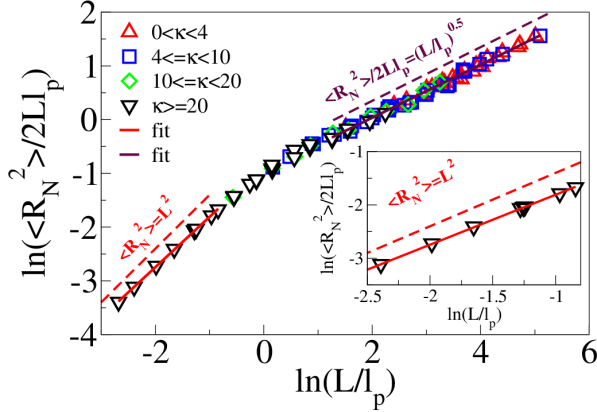


FIG. 2. $\langle R_N^2 \rangle / (2L\ell_p)$ as a function of L/ℓ_p obtained from different combination of chain length N and stiffness parameter κ (log-log scale). The solid (maroon) line is a fit to the formula $\langle R_N^2 \rangle / 2L\ell_p \sim (L/\ell_p)^{0.5}$ for $4 < L/\ell_p < 160$. The inset shows the same for small values of $0 < L/\ell_p < 1$ which clearly indicates that limiting slope of unity ($\langle R_N^2 \rangle = L^2$) for $L/\ell_p \rightarrow 0$.

in experiments with single stranded DNA on modified graphite substrate [6].

• *Monomer dynamics:* We now present BD simulation results to confirm our scaling theory. Results for $g_1(t)$, $g_2(t)$, and $g_3(t)$ shown in Fig. 3 unambiguously confirm our predictions. These plots quite clearly show three distinct scaling regimes of $g_1(t) \sim t^{0.75}$ crossing over to $g_1(t) \sim t^{0.6}$ and then merging with $g_3(t) \sim t$ at late times. The double crossover required simulation of reasonably large chain lengths ($N = 512 - 1024$) below which it is hard to see these crossovers conclusively. Fig. 4 shows plot of $g_1(t)/\ell_p^2$ as a function of rescaled time t/ℓ_p^3 which shows data collapse for various chain length N and κ again confirming the time scales for these crossovers. As

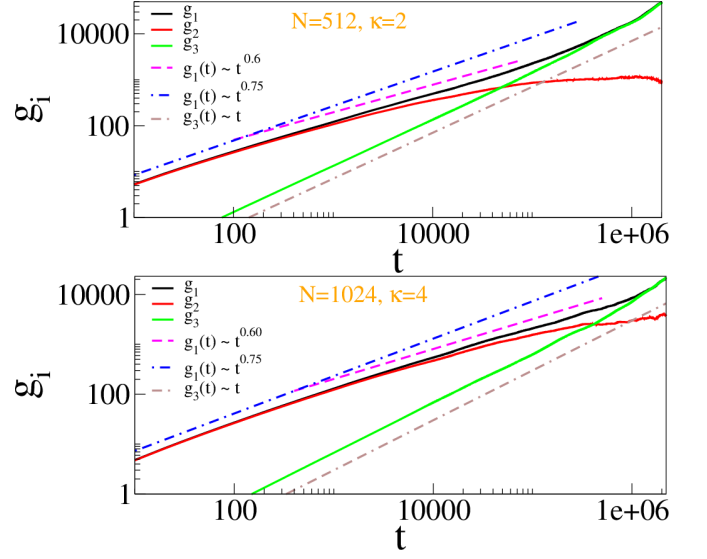


FIG. 3. (top) Plot for $g_1(t)$ (black), $g_2(t)$ (red) and $g_3(t)$ (green) as a function of time on a log-log scale for chain length $N = 512$ and $\kappa = 2.0$. The blue and magenta dashed lines correspond to straight lines $g_1(t) = At^{0.75}$, and $g_1(t) = Bt^{0.60}$, respectively, where A and B are constants. (bottom) same but for $N = 1024$ and $\kappa = 4.0$.

expected, the crossovers are rather gradual, spread out over a decade in time t each, and hence for chains that are not long enough the existence of these regimes is easily missed.

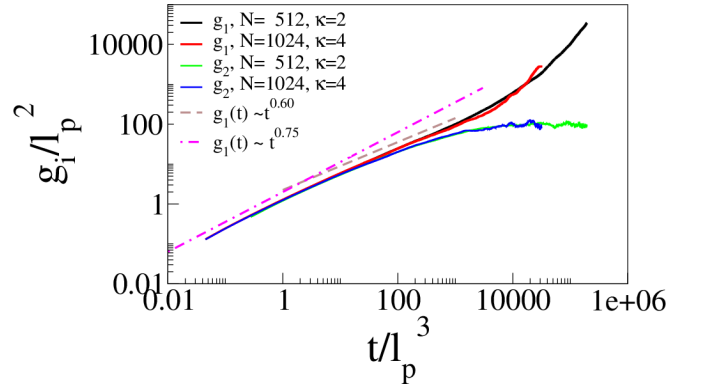


FIG. 4. Plot for $g_1(t)/\ell_p^2$ (black and red) and $g_2(t)/\ell_p^2$ (blue and green) as a function of t/ℓ_p^3 on a log-log scale for chain lengths $N = 512$, $\kappa = 2.0$ and for $N = 1024$, $\kappa = 4.0$ respectively. The dot-dashed lines correspond to slopes 0.75 (magenta) and 0.6 (brown) respectively.

To summarize, we have provided a new scaling theory of monomer dynamics for semiflexible polymers in 2D. Our theory predicts novel crossover dynamics at an intermediate time when the fluctuations of the monomers become greater than ℓ_p . Around this time the monomer dynamics becomes the same as that of a fully flexible chain characterized by $g_1(t) \sim t^{2\nu/(1+2\nu)} = t^{0.6}$ in 2D. The

theory expands the existing scaling theory for monomer dynamics for a WLC and that of a fully flexible chain to include the effect of the chain persistence length. Fully flexible chains are self-similar objects, while a polymer segment up to its own persistence length is not. Therefore, it is expected that for length scale up to ℓ_p the dynamics will have different characteristics due to bending modes arising out of the chain stiffness. The EV effect is almost negligible for the $t^{0.75}$ regime and therefore, our result is the same as that of from previous studies using WLC Hamiltonian [14, 15]. For the $t^{0.6}$ regime originating from EV effect, where the monomer dynamics is governed by Rouse relaxation of a fully flexible chain, our theory elucidates the exact role of chain persistence length neither contained in WLC model nor seen before. We also validate our new scaling theory by extensive BD simulation results.

We now comment on generalization of our results in 3D and/or in presence of hydrodynamic(HD) interactions. In the free draining limit the $t^{0.75}$ regime will remain the same in 3D [14, 15], but the intermediate Rouse relaxation regime will be characterized by $t^{2\nu/(1+2\nu)} = t^{0.54}$ ($\nu = 0.59$ in 3D). Replacing Rouse relaxation by Zimm relaxation one immediately sees that in presence of HD interaction the intermediate regime is characterized by $\sim t^{2\nu/3\nu} = t^{2/3}$ [32]. Notice that in this case ν cancels out and this relaxation should be the same in 2D and 3D. Our results are completely consistent with the observed $t^{0.5}$ and $t^{2/3}$ power laws due to Rouse and Zimm relaxation for the monomers in double and single stranded DNA using fluorescence correlation spectroscopy by Shusterman *et al.* [5].

Finally, we provide plausible explanation why this double crossover has not been seen in single molecule experiments with biopolymers [2–5]. A simple calculation for Fig. 1 shows that in order for the width of the $t^{0.75}$ and $t^{0.60}$ to be equal (in logarithmic scale) one needs $N = \ell_p^{2.2}$ in 2D. In other words for a stiffer chain one needs a very long chain to see the $t^{0.60}$ regime. Indeed in our simulation we found (not shown here) that for $\kappa = 16, 32$, and 64 , the results with chain length up to $N = 512$ are largely dominated by the $t^{0.75}$ regime and we did not clearly see the $t^{0.60}$ regime. It is only after we lowered the value of κ and used longer chain ($N = 1024$), we identified these two regimes quite conclusively (Fig. 3). We suspect that the same might happen in experiments [2]. For extreme stiff chains the $t^{0.6}$ (or $t^{0.54}$ in 3D) region can be extremely narrow and could either be easily missed or the rather smooth double crossover might be mistakenly interpreted as a single crossover (with $t^{2/3}$ in 2D). Therefore, we believe that these results will not only promote new experiments but will be extremely valuable in identifying and interpreting different scaling regimes for the monomer dynamics of semiflexible polymers.

AB, AH, and RA acknowledge financial support

through a seed grant from UCF.

-
- * Author to whom the correspondence should be addressed; aniket@physics.ucf.edu
- [1] R. Phillips, J. Kondev, and J. Theriot, *Physical Biology of the Cell*, (Garland Science, 2009).
 - [2] M. A. Dichtl and E. Sackmann, *New Journal of Physics*, **1**, 18 (1999).
 - [3] L. Le Goff, O. Hallatschek, E. Frey, and F. Amblard, *Phys. Rev. Lett.* **89**, 25801 (2002).
 - [4] A. Caspi, M. Elbaum, R. Granek, A. Lachish, and D. Zbaida, *Phys. Rev. Lett.* **80**, 1106 (1998).
 - [5] R. Shusterman, S. Alon, T. Gavrinov, O. Krichinsky, *Phys. Rev. Lett.* **92**, 048303 (2004).
 - [6] K. Rechendorff, G. Witz, J. Adamik, and G. Dietler, *J. Chem. Phys.* **131**, 095103 (2009).
 - [7] M. Rubinstein and R. H. Colby, *Polymer Physics*, (Oxford University Press, 2003).
 - [8] M. Doi and S. F. Edwards, *Theory of Polymer Dynamics*, (Clarendon Press, Oxford 1986).
 - [9] L. D. Landau and E. M. Lifshitz, *Statistical Physics, Part 1* (Pergamon Press, 3rd edition).
 - [10] H. Yamakawa, *Modern theory of polymer solution*, (Harper & Row publisher, 1971).
 - [11] L. Harnau, R. G. Winkler, and P. Reineker, *EPL* **45**, 488 (1999).
 - [12] L. Harnau, R. G. Winkler, and P. Reineker, *J. Chem. Phys.* **104**, 6355 (1996).
 - [13] R. G. Winkler, *J. Chem. Phys.* **118**, 2919 (2003).
 - [14] R. Granek, *J. Phys. II (Paris)* **7**, 1767 (1997).
 - [15] E. Farge and A. C. Maggs, *Macromolecules* **26**, 5041 (1993).
 - [16] K. Kroy and E. Frey, *Phys. Rev. E* **55**, 3091 (1997).
 - [17] J. Wilhelm and E. Frey, *Phys. Rev. Lett.* **77**, 2581 (1996).
 - [18] J. T. Bullerjahn, S. Sturm, L. Wolff and K. Kroy, *EPL* **96**, 48005 (2011).
 - [19] M. Bulacu and E. van der Giessen, *J. Chem. Phys.* **123**, 114901 (2005).
 - [20] M. O. Steinhauser, J. Schneider, and A. Blumen, *J. Chem. Phys.* **130**, 164902 (2009).
 - [21] H-P Hsu, W. Paul, and K. Binder, *EPL* **95**, 68004 (2011).
 - [22] H-P Hsu, W. Paul, and K. Binder, *EPL* **92**, 28003 (2010).
 - [23] D. W. Schaefer, J. F. Joanny, and P. Pincus, *Macromolecules* **13**, 1280 (1980).
 - [24] H. Nakanishi, *J. Physique* **48**, 979 (1987).
 - [25] G. S. Grest and K. Kremer, *Phys. Rev. A* **33**, 3628 (1986).
 - [26] I. Geroff, A. Milchev, W. Paul, and K. Binder, *J. Chem. Phys.* **33**, 6526 (1992).
 - [27] A. Milchev, W. Paul, and K. Binder, *J. Chem. Phys.* **99**, 4786 (1993).
 - [28] K. Binder and W. Paul, *J. Polym. Sc. B*, **35**, 1 (1997).
 - [29] R. Adhikari and A. Bhattacharya, *J. Chem. Phys.* **138**, 240909 (2013).
 - [30] See Supplemental Material at <http://link.aps.org> for further details about the model and BD simulation details.
 - [31] H-P Hsu, W. Paul, and K. Binder, *Macromolecules* **43**, 3094 (2010).
 - [32] M. Hinczewski, X. Schlagberger, M. Rubinstein, O. Krichinsky, and R. R. Netz, *Macromolecules* **42**, 860 (2009).

Universal monomer dynamics of a two dimensional semi-flexible chain: Supplemental Materials

Aiqun Huang, Ramesh Adhikari, and Aniket Bhattacharya

Department of Physics, University of Central Florida, Orlando, Florida 32816-2385, USA

Kurt Binder

Institut für Physik, Johannes Gutenberg-Universität Mainz, Staudinger Weg 7, 55099, Mainz, Germany

(Dated: Aug 09, 2013)

THE MODEL AND DETAILS OF BROWNIAN DYNAMICS SIMULATION

We have carried out Brownian dynamics (BD) simulation using a bead spring model for a semiflexible polymer chain (Fig. 1) with excluded volume (EV), spring and bond bending potentials as described below [1]. The excluded volume interaction between any two monomers is given by short range Lennard-Jones (LJ) potential.

$$U_{\text{LJ}}(r) = 4\epsilon \left[\left(\frac{\sigma}{r} \right)^{12} - \left(\frac{\sigma}{r} \right)^6 \right] + \epsilon \text{ for } r \leq 2^{1/6}\sigma$$

$$= 0 \text{ for } r > 2^{1/6}\sigma . \quad (1)$$

Here, σ is the effective diameter of a monomer, and ϵ is the strength of the potential. The connectivity between neighboring monomers is modeled as a Finite Extensible Nonlinear Elastic (FENE) spring with

$$U_{\text{FENE}}(r) = -\frac{1}{2}kR_0^2 \ln(1 - r^2/R_0^2) , \quad (2)$$

where r is the distance between consecutive monomers, k is the spring constant, and R_0 is the maximum allowed separation between connected monomers [1]. The chain stiffness is introduced by adding an angle dependent interaction between successive bonds (discrete worm-like-chain potential) as

$$U_{\text{BEND}}(\theta_i) = \kappa(1 - \cos \theta_i). \quad (3)$$

Here θ_i is the angle between the bond vectors $\vec{b}_{i-1} = \vec{r}_i - \vec{r}_{i-1}$ and $\vec{b}_i = \vec{r}_{i+1} - \vec{r}_i$, respectively, as shown in Fig. 1. The strength of the interaction is characterized by the bending rigidity κ .

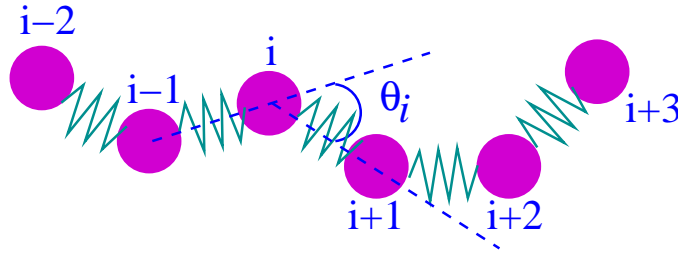


FIG. 1. Bead-spring model of a polymer chain with bending angle θ_i subtended by the vectors $\vec{b}_i = \vec{r}_i - \vec{r}_{i-1}$ and $\vec{b}_{i+1} = \vec{r}_{i+1} - \vec{r}_i$.

We use the Brownian dynamics with the following equation of motion for the i^{th} monomer

$$m\ddot{\vec{r}}_i = -\vec{\nabla}(U_{\text{LJ}} + U_{\text{FENE}} + U_{\text{BEND}}) - \zeta\dot{\vec{r}}_i + \vec{\eta}_i. \quad (4)$$

Here ζ is the monomer friction coefficient and $\vec{\eta}_i(t)$, is a Gaussian white noise with zero mean at a temperature T , and satisfies the fluctuation-dissipation relation:

$$\langle \vec{\eta}_i(t) \cdot \vec{\eta}_j(t') \rangle = 4k_B T \zeta \delta_{ij} \delta(t - t'). \quad (5)$$

The reduced units of length, time and temperature are chosen to be σ , $\sigma\sqrt{\frac{m}{\epsilon}}$, and ϵ/k_B respectively. For the spring potential we have chosen $k = 30$ and $R_0 = 1.5\sigma$, the friction coefficient $\zeta = 0.7$, and the temperature $T = 1.2/k_B$. The choice of the FENE potential along with the LJ interaction parameters ensures that the average bond-length in the bulk $\langle b_l \rangle = 0.971$. With the choice of these parameters the probability of chain crossing is very low. The LJ and the FENE parameters are chosen to be the same as in our previous studies of polymer translocation of semiflexible chains [2]. We advance the position coordinates using a reduced time step $\Delta t = 0.01$ following the algorithm proposed by van Gunsteren and Berendsen [3].

We have carried out simulation for various combinations of N (16 - 1024) and κ (1 - 100) and sampled a wide range of values of $n_p = L/\ell_p$ (please see Eqn. 2 in the main text) to simulate semiflexible chains with varying degree of stiffness. With these choices of parameters we find that the average bond-length $\langle b_l \rangle$ is hardly affected by the chain stiffness parameter. During the simulation, first we have equilibrated each chain for 5-100 times of the Rouse relaxation time, and then collected data over 30-250 times of the Rouse relaxation time in order to obtain good statistics for $g_1(t)$, $g_2(t)$, and $g_3(t)$. To calculate crossover dynamics and the exponents it took a 16-core Intel processor almost a month to finish the most time-consuming job ($N=1024$).

Using the BD algorithm we first calculated the chain persistence length ℓ_p as a function of the bending rigidity κ . It is worth noting that the persistence length must not be extracted from the decay of bond orientational correlations at large distances along the chain, but even in presence of the EV interaction it still can be estimated from the average $\langle \cos \theta \rangle$ between subsequent bonds by the standard formula $\ell_p = -1/\ln(\langle \cos \theta \rangle)$. We find that this estimate also coincides with the continuum theory result $\ell_p = 2\kappa/k_B T$ [4] as shown in Fig. 2(a) where we have used $\langle \cos \theta \rangle$ obtained from simulation to calculate ℓ_p for different combination of κ and N . Since persistence length is an intrinsic local property of the chain, EV has very little effect on it. This although not the main focus of this letter is a new result [7]. Using ℓ_p obtained from simulation we then verified that in 2D the end-to-end distance satisfies the relation $\sqrt{\langle R_N^2 \rangle} \sim N^\nu \ell_p^{0.25}$ [5, 6] for various combinations of ℓ_p and chain length N [2] as shown in Fig 2(b). We have used these values of ℓ_p and $\sqrt{\langle R_N^2 \rangle}$ in the main text.

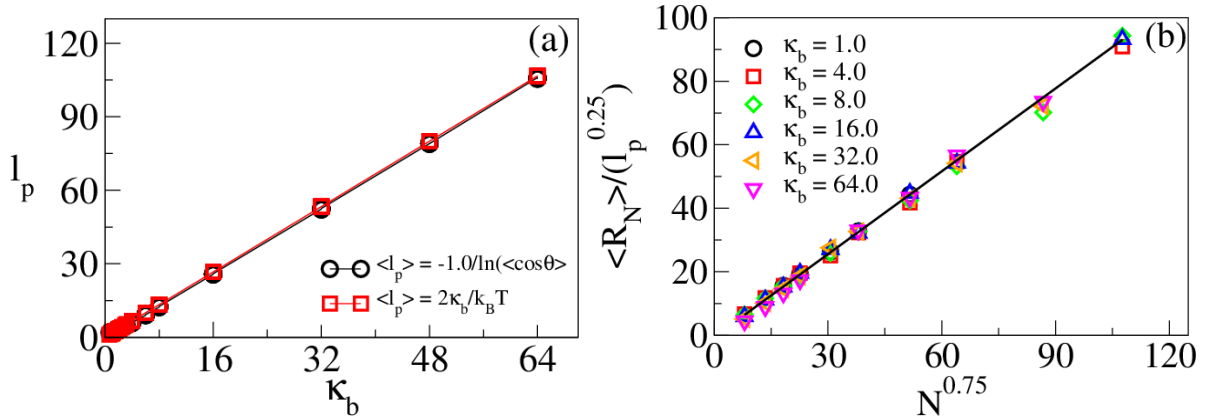


FIG. 2. (a) Comparison of $\ell_p = -1/\ln(\langle \cos \theta \rangle)$ and $\ell_p = 2\kappa/k_B T$. (b) Plot of $\sqrt{\langle R_N^2 \rangle}/\ell_p^{0.25}$ versus $N^{0.75}$ for various values of the chain stiffness parameter. All the data for different stiffness parameters collapse on the same master plot. The solid line is a fit to a straight line

-
- [1] G. S. Grest and K. Kremer, Phys. Rev. A **33**, 3628 (1986).
 - [2] R. Adhikari and A. Bhattacharya, J. Chem. Phys. **138**, 240909 (2013)
 - [3] W. F. van Gunsteren and H. J. C. Berendsen, Mol. Phys. **45**, 637 (1982).

- [4] M. Rubinstein and R. H. Colby, *Polymer Physics*, (Oxford University Press, 2003).
- [5] D. W. Schaefer, J. F. Joanny, and P. Pincus, *Macromolecules* **13**, 1280 (1980).
- [6] H. Nakanishi, *J. Physique* **48** 979 (1987).
- [7] It is worth mentioning that a very common used definition of persistence length in the literature is $\langle \vec{b}_1 \cdot \vec{R}_N \rangle$ [8, 9] and has been used in simulations [10]. An end-to-end vector can not be a good candidate to explore local property of a chain, especially for long chains [11]. We have checked that this definition does not simply work and is somewhat misleading.
- [8] S. Redner and V. Privman, *J. Phys. A: Math. Gen.* **20**, L857 (1987).
- [9] H. Yamakawa, *Modern theory of polymer solution*, (Harper & Row publisher, 1971).
- [10] P. Cifra, *Polymer* **45**, 5995 (2004).
- [11] H-P Hsu, W. Paul, and K. Binder, *Macromolecules* **43** 3094 (2010).